

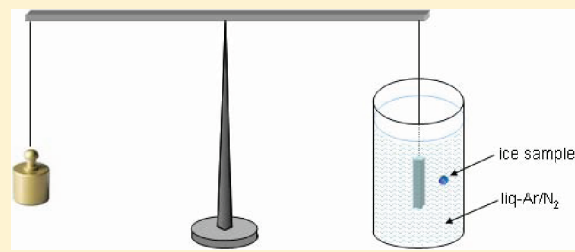
Cryoflotation: Densities of Amorphous and Crystalline Ices

Thomas Loerting,^{*†} Marion Bauer,[‡] Ingrid Kohl,[‡] Katrin Watschinger,[†] Katrin Winkel,^{†,‡} and Erwin Mayer^{†,§}

[†]Institute of Physical Chemistry and [‡]Institute of General, Inorganic and Theoretical Chemistry, University of Innsbruck, Innrain 52a, A-6020 Innsbruck, Austria

[†]Division of Biological Chemistry, Biocenter, Innsbruck Medical University, Fritz-Pregl-Strasse 3, A-6020 Innsbruck, Austria

ABSTRACT: We present an experimental method aimed at measuring mass densities of solids at ambient pressure. The principle of the method is flotation in a mixture of liquid nitrogen and liquid argon, where the mixing ratio is varied until the solid hovers in the liquid mixture. The temperature of such mixtures is in the range of 77–87 K, and therefore, the main advantage of the method is the possibility of determining densities of solid samples, which are unstable above 90 K. The accessible density range (~ 0.81 – 1.40 g cm^{-3}) is perfectly suitable for the study of crystalline ice polymorphs and amorphous ices. As a benchmark, we here determine densities of crystalline polymorphs (ices I_h, I_c, II, IV, V, VI, IX, and XII) by flotation and compare them with crystallographic densities. The reproducibility of the method is about $\pm 0.005 \text{ g cm}^{-3}$, and in general, the agreement with crystallographic densities is very good. Furthermore, we show measurements on a range of amorphous ice samples and correlate the density with the *d* spacing of the first broad halo peak in diffraction experiments. Finally, we discuss the influence of microstructure, in particular voids, on the density for the case of hyperquenched glassy water and cubic ice samples prepared by deposition of micrometer-sized liquid droplets.



INTRODUCTION

The mass density, defined as mass per unit volume, is an important quantity used to characterize materials. It typically increases upon pressure increase but decreases upon temperature increase. When measured as a function of temperature and pressure, the equation of state can be constructed from density data. Jumps in density incurred upon changing pressure and/or temperature indicate first-order phase transitions.¹ Density is, hence, an important quantity not only in material science but also in thermodynamics. In the case of fluids, some methods have been developed in the last 30 years for accurately measuring (*p*, ρ , *T*) data for constructing the thermodynamic surface.^{2,3} For instance Wagner et al. have constructed single- and two-sinker densimeters for gases and liquids based on the Archimedes buoyancy principle,⁴ which can be employed in wide pressure (up to 30 MPa), temperature (60–523 K), and density ranges (0.0007–2 g cm⁻³).^{5–7} Other densimeters aimed at measuring gas and liquid densities employed in the past are piezometers,^{8,9} vibrating bodies,¹⁰ hydrostatic balances,¹¹ and magnetic suspension densimeters.^{12–17} The density of solids is typically measured simply by weighing them and determining their volume. The latter can be done by measuring well-defined dimensions in objects of simple geometry. Alternatively, it can be measured by fully immersing the solid in a liquid of known density, typically water, and measuring the buoyant force using a balance (hydrostatic balance). Also, the use of gravimetric techniques, for example, by employing pycnometers, is possible. Such measurements are often limited to ambient temperature and affected by many unwanted effects, for example, solubility of the

solid in the liquid medium or other types of interaction between the liquid medium and the solid. Some pycnometers can be filled with liquefied gases at low temperature instead of water. This allows measurements of solid densities not only at ambient temperature but also below room temperature.¹⁸ An approach that does not require a liquid medium, gravimetry or volumetry, is nowadays very common. In the case of crystalline substances, the density is determined from diffraction experiments in the course of the crystal structure determination, often even as a function of temperature. The density can either be determined using *in situ* experiments at elevated pressure or *ex situ* experiments at (or near) ambient pressure. Both single-crystal and powder diffraction experiments are employed for this purpose. Unfortunately, the crystallographic approach to the mass density cannot be employed in a straightforward way in the case of noncrystalline (glassy, amorphous, fluid) samples. However, some techniques involving extrapolation of the structure factor to obtain densities have been developed, which allow for determination of densities from *ex situ* or *in situ* diffraction data.^{19–22}

Amorphous ices of differing densities are supposed to be the most common form of ice in space.^{23–31} Knowledge of densities of different variants of amorphous ices is highly desirable because

Special Issue: H. Eugene Stanley Festschrift

Received: May 22, 2011

Revised: July 25, 2011

Published: August 31, 2011

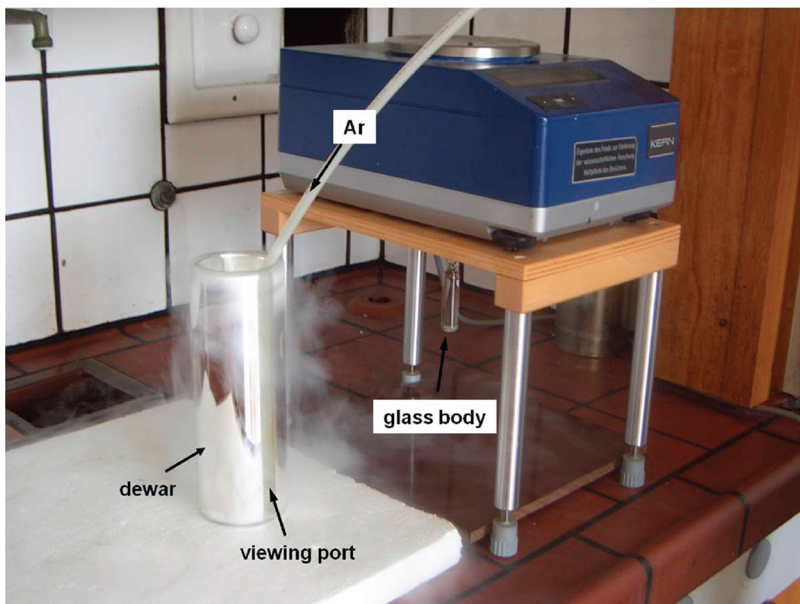


Figure 1. Experimental setup showing the reflective-coated glass dewar with a viewing port, the hose connected to the argon cylinder, the underfloor balance, and the calibrated glass body hanging beneath the balance (Kern, model 810/23).

the proposal by H. Eugene Stanley et al.^{32–49} of a phase transition between a low-density form and a high-density form of noncrystalline water has been considered to explain many anomalous properties of water over the last 20 years. Experimental determination of the mass density of amorphous ice samples is a challenge, though, both because these samples are instable at ambient temperature and because they are noncrystalline. A method is required in which the amorphous ice sample temperature never exceeds ~ 100 K, especially because some of the amorphous ice samples transform only slightly above 100 K. In particular, the onset of the transformation from high-density amorphous ice (HDA) to low-density amorphous ice (LDA) is known to occur at about 100 K.^{50,51} Some scattered results reporting densities of amorphous ice are found in the literature, which include the use of cryoliquids^{52,53} and diffraction methods.¹⁹ However, no comprehensive set of density data on amorphous and crystalline ice is available, which is obtained using a single method and hence allows for direct comparison of densities. Therefore, it has been the aim of our work to develop a technique for measuring solid-state densities at cryotemperatures.

■ EXPERIMENTAL SECTION

Method of Measuring Density. The experimental setup is shown in Figure 1, and the principle of the method is illustrated schematically in Figure 2. An ice sample, usually a piece of about 100 mg, is placed inside of a dewar filled with filtered (ice-free) liquid nitrogen. We employ a glass dewar (isotherm, 6 cm inner diameter, 20 cm height) with a reflective coating and a viewing port. The dewar is placed on some thermally insulating material, for example, styrofoam, in order to prevent vigorous boiling of liquid nitrogen. The ice sample immediately sinks to the bottom because its density exceeds the density of liquid nitrogen of 0.808 g cm^{-3} . Subsequently, we carefully bubble gaseous argon (argon5.0) through the liquid nitrogen, typically at a flow rate of a few mL per second. Some of the argon liquefies because its boiling point (87.28 K) is 10 K higher than nitrogen's boiling

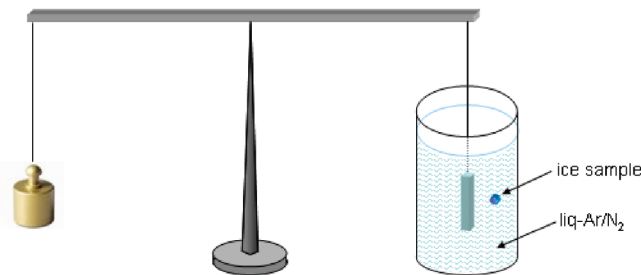


Figure 2. Scheme illustrating the principle of Archimedes. In the case of a hovering ice sample, the density of the cryomixture equals the density of the ice sample. The density of the cryomixture, and hence that of the ice sample, can be determined by measuring the apparent reduction of mass (because of the buoyant force) of a body of known volume fully immersed in the cryomixture compared to the true mass of the same body measured in air.

point (77.35 K). A homogeneous argon–nitrogen mixture results, in which the mole fraction of argon constantly increases as long as argon is bubbled through the mixture. The density of liquid argon is 1.397 g cm^{-3} , and therefore, the density of the mixture constantly increases. Also, the temperature of the gently boiling mixture slowly increases as a result of the increasing argon fraction. (In theory, an exact measurement of temperature could even replace measurement of the density of the mixture because there is a well-defined relationship between the boiling temperature and density of the mixture. However, in practice, the accuracy and reproducibility of densities determined from boiling temperature measurements turned out to be rather low.) After some time of bubbling, the ice sample will lift from the bottom, move to the top, and float at the surface. This indicates that the density of the cryomixture now exceeds the density of the ice sample. By adding a small volume of liquid nitrogen, the ice sample will slowly sink again. The density of the mixture can be fine-tuned by alternately bubbling a small volume of gaseous argon through the mixture and adding a small volume of liquid

nitrogen. This corresponds to a “density titration”.⁵⁴ While monitoring the sample through the viewing port, the density is fine-tuned in this manner as long as the sample hovers in the mixture without moving up- or downward. According to Archimedes’ principle, levitation of the ice sample in the cryomixture as depicted in Figure 2 implies equality of the densities of the ice sample and the cryomixture.

At this point, the task of measuring the density of the ice sample can be achieved by measuring the density of the liquid cryomixture. This can be reached in several ways. In the initial stages of the work, we employed a set of nine aerometers for this purpose (0.880–0.940, 0.940–1.000, 1.000–1.060, 1.060–1.120, 1.120–1.180, 1.180–1.240, 1.240–1.300, 1.300–1.360, 1.360–1.420 g cm⁻³). The scale reading of these aerometers is divided in units of ± 0.001 g cm⁻³, and we found reproducibility of the density reading in the same cryomixture of ± 0.001 –0.002 g cm⁻³. These aerometers are calibrated by the company at a temperature of 293 K, and therefore, the densities of cryomixtures at 77–87 K read from the aerometer differ systematically from the real density. This necessitates calibration of the aerometer readings by measuring the density of the cryomixture using another method or by measuring the density of a solid of known density at 80 K. The systematic error due to the temperature difference turned out to be quite small, for example, -0.0025 g cm⁻³ in the case of the aerometer for the density range of 0.880–0.940 g cm⁻³. In terms of accuracy, the aerometers are suitable for measuring absolute densities to better than 0.005 g cm⁻³. However, it turned out that use of aerometers in cryomixtures suffers from one major drawback: they break or burst after a few measurements. Instead of using aerometers, we then resorted to underfloor buoyancy weighing of a calibrated glass body (see Figure 1) immersed in a liquid on a high-precision balance (Kern model 810/23). Full immersion of the glass body in a liquid causes a buoyant force and an apparent reduction of the mass Δm in comparison to the unimmersed body. The density ρ of the liquid can be calculated from $\rho = \Delta m/V$ if the volume of the glass body and hence the volume of the displaced liquid are known. The glass body is made of borosilicate glass, which has a very low coefficient of thermal expansion of 2.8×10^{-6} K⁻¹ in the range of 200–300 K and is even lower in the range of 77–200 K. In total, this glass body contracts by only 0.05% upon cooling from ambient to liquid nitrogen temperature. We determined a glass body volume of 10.01 cm³ at 293 K in water and 10.00 cm³ at 77 K in liquid nitrogen, which includes the volume of the submerged fraction of the thin wire (of about 1 cm in length) used for affixing the glass body to the underfloor weighing hook of the balance. Before immersing the glass body in cryomixtures of argon and nitrogen, it is necessary to precool the glass body to 77 K in liquid nitrogen. Immersing the warm glass body directly in the cryomixture would result in strong boiling and change of the mixing ratio. It is also necessary to be quick when changing the glass body from liquid nitrogen to the cryomixture. If it were hanging for prolonged periods in humid air, ice would condense on the precooled glass body (at 77 K) and increase its volume slightly. The reproducibility of the reduction of mass Δm measured for one specific cryomixture has turned out to be ± 0.005 g, corresponding in terms of density to ± 0.0005 g cm⁻³. Please note, however, that the reproducibility is about ± 0.002 –0.005 g cm⁻³ for different cryomixtures, in which one specific piece of ice has been brought to levitation in a sequence of flotation experiments. The reproducibility of the density for different pieces of ice from the same sample has also been found to be ± 0.002 –0.005 g cm⁻³. Thus, all densities

quoted in this work show a random error of ± 0.002 –0.005 g cm⁻³. We also investigated the influence of the shape (spherical, long, flat) and mass (10–500 mg) of the piece of ice and found that all sizes and shapes show identical densities within the error quoted above. However, one issue has appeared especially for quite flat pieces of hyperquenched glassy water. These pieces show some tendency to stick to the dewar walls, most likely due to electrostatic charging. These samples can be freed from the wall using a discharge gun (spark tester). Whether or not there is a systematic error is analyzed by measuring ice polymorphs of known crystallographic density (see Results).

Sample Preparation. Bubble-free hexagonal ice was prepared by repeated freeze–thaw cycles of ~ 10 mL of deionized water. The freeze–thaw cycles were done in a glass flask connected to a rotary pump. First, the flask was immersed in liquid nitrogen, which resulted in freezing to hexagonal ice. Then, the flask was pumped to ~ 10 mbar, and the liquid nitrogen bath was removed. Gas bubbles, which were pumped off, were clearly visible in the course of slow melting. As soon as boiling of the molten ice was starting, the flask was immersed in liquid nitrogen again. After three or four such freeze–thaw cycles, the hexagonal ice was perfectly clear, with no trapped bubbles, and gas bubbles were no longer seen upon melting.

Hyperquenched glassy water (HGW) was prepared by ultrafast cooling of 5 μm in diameter droplets to 77 K, as described earlier in our previous work.⁵⁵ The diameter of the aperture through which droplets enter the vacuum chamber was varied between 100 and 400 μm . Also, the droplet diameter was changed to 3 μm in diameter for one sample. The aperture size determines the rate at which droplets hit the cooled sample holder made from copper. As described in ref 55, deposition times required to produce approximately equivalent amounts of sample are 37 min for a 200 μm aperture and 16 min for 300 μm . In addition to these two apertures described in ref 55, we employed additional ones here. Use of the 400 μm aperture reduced deposition times to 9 min, and use of 100 and 150 μm apertures increased the deposition time to 150 and 70 min, respectively. The base pressure in the vacuum chamber was 5×10^{-8} – 1×10^{-9} mbar, which increased during droplet deposition to 4×10^{-2} (400 μm), 8×10^{-4} (300 μm), 4×10^{-4} (200 μm), 1×10^{-5} (150 μm), or 4×10^{-6} mbar (100 μm). Characterization of the samples by differential scanning calorimetry and powder X-ray diffraction is shown in ref 55 for deposits obtained using the 200 and 300 μm aperture. We emphasize that the deposits obtained here using other aperture sizes show highly similar thermograms and diffractograms. The ultrastructure of such deposits as visualized by electron microscopy with the freeze etching and shadowing technique is shown as Figure 2 in ref 55. These images clearly show gaps and cavities, which were opened by fracturing the samples. The samples were freeze-fractured at ~ 165 K, and therefore, crystallization to cubic ice occurred. Despite crystallization to cubic ice in the preparation procedure for the electron microscopy images, slightly squeezed 3 μm droplets can be clearly identified in the image. That is, HGW samples show cavities and gaps in between droplets. The size and volume of these cavities and gaps remain unaffected by crystallizing the glassy sample.

Cubic ice was prepared in the same way as hyperquenched glassy water, with the one difference that the sample holder was kept at 190 K rather than at 77 K.⁵⁶ Powder X-ray diffractograms and thermograms of cubic ice are shown in ref 56. We emphasize that this type of cubic ice samples shows a high cubicity index

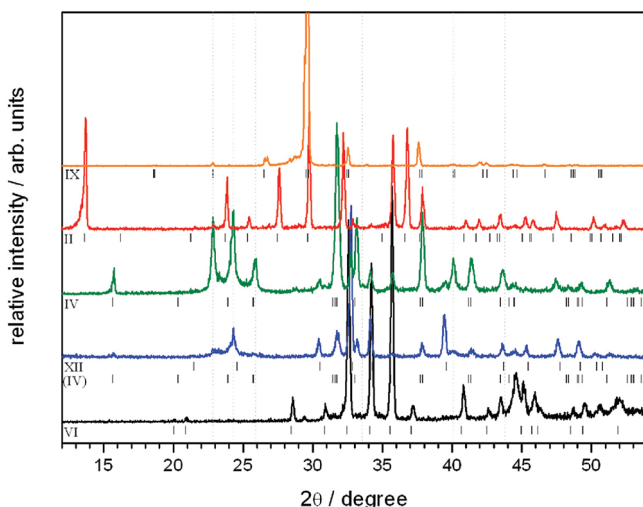


Figure 3. Powder X-ray diffractograms of high-density ($\rho > 1 \text{ g cm}^{-3}$) ice polymorphs listed in Table 1. The diffractograms are recorded on a Siemens D5000 diffractometer ($\text{Cu K}\alpha_1$) in $\theta-\theta$ arrangement at $\sim 85 \text{ K}$ using an Anton-Paar chamber and a Goebel mirror.

and, correspondingly, only a small amount of hexagonal stacking faults.^{57,58} This is evidenced by an intensity of the hexagonal (100) Bragg peak, which is approximately 1/4 of the intensity of the cubic (111) Bragg peak.

High-pressure ice polymorphs were prepared in a piston cylinder apparatus with a bore of 10 mm in diameter. Cylindrical samples of typically 500 mg were prepared by freezing hexagonal ice and then employing pressure-induced amorphization to unannealed high-density amorphous ice (uHDA) at 77 K,⁵³ followed by isobaric crystallization. Ice II and ice IX were crystallized from uHDA at 0.28 GPa by heating to 210 and 250 K, respectively.⁵⁹ Ice XII and ice VI were crystallized at 1.08 GPa by heating to 180 and 220 K at 10 K/min, respectively.^{60,61} Ice V was prepared by heating uHDA at 0.51 GPa to 250 K.⁵⁹ Ice IV was prepared by crystallizing uHDA at 0.81 GPa at a rate of 1 K/min.^{61,62} Contamination of the samples with other high-pressure polymorphs was checked by powder X-ray diffraction, as depicted in Figure 3. This is especially important because parallel crystallization kinetics is known to occur, for example, to ice IV and ice XII at 0.81 GPa, where the relative amount is governed by the heating rate.⁶²

Also, amorphous ices were prepared in a piston cylinder apparatus. HDA states were prepared in two ways, (i) by pressure-induced amorphization of hexagonal ice at 77 K and $>1.0 \text{ GPa}$ (uHDA) according to the procedure developed by Mishima et al.⁵³ and (ii) by decompression of very high-density amorphous ice (VHDA) at 140 K to a select pressure according to the procedure developed by Winkel et al.⁶³ VHDA itself is prepared by heating the uHDA obtained using route (i) to 165 K at 1.1 GPa according to the procedure developed by Loerting et al.⁶⁴ LDA was prepared by heating uHDA to $\sim 150 \text{ K}$ at 0.013 GPa.

Cryoflotation was done typically on three or four sample pieces, and the reproducibility was found to be $\pm 0.005 \text{ g cm}^{-3}$ in most cases. In the remaining cases, the reproducibility was much worse, for example, $\pm 0.04 \text{ g cm}^{-3}$. We could attribute the much worse reproducibility in these cases to heterogeneity of the sample by analyzing the powder X-ray diffractograms. For instance, a heterogeneous sample containing ice V and ice IX

Table 1. Densities of Polycrystalline Ice Samples as-measured by Cryoflotation in Liquid N₂/Ar^a

| substance | contamination | density by flotation (77–87 K, 1 bar) | crystallographic density (1 bar) |
|--|---------------|--|--|
| ice I _h | | 0.932 | 0.934 (85 K) ^{65,67} 0.933 (73 K) ⁶⁸ 0.931 (143 K) ⁸³ |
| ice I _c | | 0.943 | 0.931 (78 K) ⁵⁷ (see Table 4) |
| ice IX | | 1.169 | 0.934 (143 K) ^{83–85} 1.160 (98 K) ⁷⁴ 1.167 (110 K) ⁷³ 1.162 (110 K) ⁷¹ |
| ice II | | 1.211 | 1.170 (123 K) ⁸⁶ |
| ice IV | 5% ice XII | 1.291 | 1.272 \pm 0.005 (110 K) ⁷⁹ |
| ice XII | 15% ice IV | 1.268 | 1.30 (127 K) ⁸¹ |
| ice VI | | 1.335 | 1.314 (98 K) ⁷⁶ |
| ice V | | 1.249 | 1.231 (98 K) ⁷⁵ |
| naphthalene (C ₁₀ H ₈) | | 1.228 | 1.235 (80 K) ⁶⁹ |

^a Reproducibility is $\pm 0.005 \text{ g cm}^{-3}$. The samples were checked by powder X-ray diffraction (cf. Figure 3). In the case of ice XII/IV, the contamination was estimated using PowderCell.⁸² The crystallographic density is given for comparison. Naphthalene was measured for calibration. Except for ice I_h and ice I_c, the densities were measured from one or two single pieces of ice, which were floated up to three times.

in comparable amounts showed densities ranging between 1.17 and 1.25 g cm^{-3} . Data obtained from apparently heterogeneous samples are not included in the tables in the Results section.

RESULTS

Ice Polymorphs. Table 1 summarizes the densities of polycrystalline ice samples determined by cryoflotation. According to Röttger et al., the density of hexagonal ice is 0.934 g cm^{-3} at 55–85 K and 0.933 g cm^{-3} at temperatures below that interval.⁶⁵ The density decreases also above 85 K, and therefore, there is a density maximum in the vicinity of 75 K. At 265 K, the density is 0.918 g cm^{-3} . The data by Röttger et al. obtained on powdered ice I_h samples using synchrotron radiation⁶⁵ agree very well with density data deduced by Eisenberg and Kauzmann⁶⁶ on the basis of the X-ray diffraction data by La Placa and Post.⁶⁷ There is also fair agreement with the data obtained by X-ray diffraction on polycrystalline samples by Brill and Tippe,⁶⁸ even though their density of 0.933 g cm^{-3} at 73 K is slightly lower. We determine the density of hexagonal ice to be $0.932 \pm 0.002 \text{ g cm}^{-3}$, where the error quoted implies that all measured densities are within the error bar. A total of three different preparations of bubble-free hexagonal ice were made, and eight pieces of different size and shape were employed. Each piece was measured several times. The excellent agreement of our data with the data deduced from diffraction measurements of the unit cell parameters shows that our method is not only precise but also accurate. Similarly, our calibration measurement of the density of naphthalene (C₁₀H₈) at 84 K yielding a density of $1.228 \pm 0.005 \text{ g cm}^{-3}$ agrees very well with the literature density of 1.235 at 80 K.⁶⁹ That is, the method of cryoflotation in liquid Ar/N₂ mixtures results in accurate and

precise densities over a broad density range both at low and high argon content. This proves that both argon and nitrogen are indeed inert in the sense that they do not interact with the sample and change densities, at least in the case of nonporous samples.

All high-pressure polymorphs studied in our cryomixtures fall in the density range of $1.16\text{--}1.34 \text{ g cm}^{-3}$, for which the naphthalene case demonstrates accurate densities. High-pressure polymorphs are expected to be nonporous. In the procedure of quenching the samples to 77 K and releasing the pressure, we released the pressure only slowly in order to avoid formation of microcracks.⁷⁰ In case of ice IX, neutron single-crystal data,⁷¹ X-ray single-crystal unit cell data,⁷² and neutron powder data⁷³ are in good agreement and indicate a density of $1.160\text{--}1.167 \text{ g cm}^{-3}$ at $98\text{--}110 \text{ K}$. Our measured value of $1.169 \pm 0.005 \text{ g cm}^{-3}$ at $\sim 83 \text{ K}$ is in excellent agreement with the unit cell data in the literature. For ices V and VI, our density is higher than the unit cell data by Kamb et al.^{74,75} by about 0.02 g cm^{-3} . A small part of the difference may be accounted for by temperature, which is 98 K in case of Kamb et al.^{74,75} and $\sim 83 \text{ K}$ in our measurements. Unfortunately, there are no other diffraction studies in the literature on recovered samples. Other unit cell data available in the literature^{76–78} were obtained on pressurized samples and cannot be used for comparing to the ambient pressure data reported here. The analysis of the powder X-ray diffractogram does not reveal any by-phases, and therefore, the reason for the slightly higher density measured by cryoflotation remains unclear. We want to emphasize, though, that the agreement with the crystallographic data is still very good. Also, in the case of ice IV, the density measured by us is about 0.02 g cm^{-3} higher than the one determined by Engelhardt and Kamb using single-crystal X-ray diffraction.⁷⁹ The difference can be explained on the basis of different temperature (83 versus 110 K), which explains at least half of the difference, and on the basis of approximately 5% ice XII as a by-phase, which explains the remaining difference. Ice XII is known to be a byproduct when preparing ice IV by crystallizing HDA. There is a parallel crystallization kinetics, which can be governed by variation of the heating rate.^{61,62,80} Also, in the case of ice XII, we identify a byproduct, namely, $\sim 15\%$ of ice IV, in the sample used for cryoflotation. Even when considering the reduction of the measured density caused by the byproduct, we measure a density that is lower than the crystallographic density reported by Koza et al.⁸¹ by $\sim 0.03 \text{ g cm}^{-3}$. In the case of ice II, our density ($\sim 83 \text{ K}$) is higher than the single-crystal neutron diffraction density by $\sim 0.04 \text{ g cm}^{-3}$ (123 K). A side-phase cannot be identified from the powder X-ray diffractogram, and therefore, the reason for the difference may only be speculated about. In summary, the agreement between crystallographic densities and our values obtained by cryoflotation is very good. The agreement is typically better than $\pm 0.01\text{--}0.02 \text{ g cm}^{-3}$, with the exceptions of ice XII and ice II.

Hyperquenched Glassy Water (HGW). Table 2 summarizes the results on hyperquenched glassy water samples. In the course of the production, both the droplet size was changed from 5 to $3 \mu\text{m}$ and the aperture through which droplets enter the vacuum chamber was varied between 100 and $300 \mu\text{m}$. The findings for different aperture sizes are visualized in Figure 4. Most notably, we clearly notice a trend that larger aperture sizes and smaller droplet sizes result in lower densities. Change from the $100 \mu\text{m}$ aperture to the $300 \mu\text{m}$ aperture reduces the density of HGW samples by about 0.02 g cm^{-3} , and an additional reduction of 0.02 g cm^{-3} is obtained by reducing the droplet size. We explain

Table 2. Densities of Hyperquenched Glassy Water (HGW) Samples as-measured by Cryoflotation in Liquid N₂/Ar^a

| aperture/droplet diameter | HGW density (as-measured) | ice I _h Density | HGW density (corrected) |
|---------------------------------|---------------------------|----------------------------|-------------------------|
| $300 \mu\text{m}/3 \mu\text{m}$ | 0.904 | 0.895 | 0.943 |
| $300 \mu\text{m}/5 \mu\text{m}$ | 0.920 | 0.915 | 0.939 |
| | 0.922 | 0.910 | 0.946 |
| $200 \mu\text{m}/5 \mu\text{m}$ | 0.928 | 0.912 | 0.950 |
| | 0.927 | 0.913 | 0.948 |
| $150 \mu\text{m}/5 \mu\text{m}$ | 0.935 | 0.928 | 0.941 |
| $100 \mu\text{m}/5 \mu\text{m}$ | 0.945 | 0.935 | 0.944 |
| | | | 0.944 ± 0.005 |

^a Reproducibility is $\pm 0.005 \text{ g cm}^{-3}$. The samples were converted to hexagonal ice by keeping them for 15 minutes at 260 K. Correction is necessary because HGW samples contain a varying number of gaps and cavities in between glassy droplets. See text for details. In the cases of $300 \mu\text{m}/5 \mu\text{m}$ and $200 \mu\text{m}/5 \mu\text{m}$, we prepared two samples of HGW. These values are not averaged in order to demonstrate reproducibility of sample preparation.

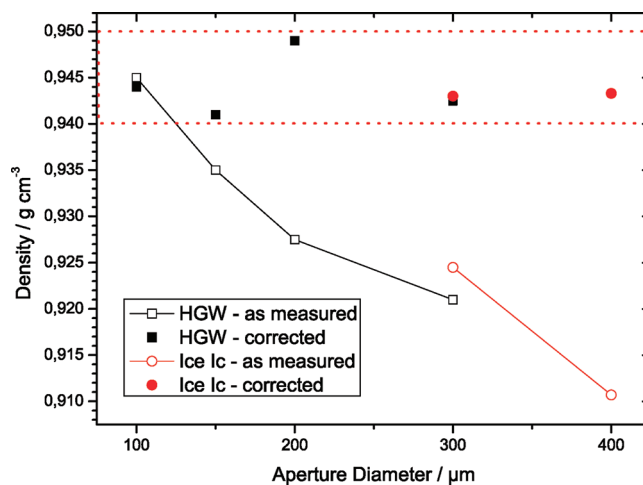


Figure 4. Influence of aperture size on as-measured (open symbols) and corrected (filled symbols) densities of hyperquenched glassy water (squares) and hyperquenched cubic ice (circles) samples. Data taken from Tables 3 and 4. Error bars are $\pm 0.005 \text{ g cm}^{-3}$. Please note that corrected densities are independent of aperture size. All of them are inside of the red dotted rectangle at $0.945 \pm 0.005 \text{ g cm}^{-3}$.

this finding by considering voids inside of the sample, which are inaccessible for argon and nitrogen. Squeezed droplets and gaps and cavities in between the droplets are clearly visible in electron microscopy images of freeze-fractured HGW samples even after crystallization to cubic ice.⁵⁵ The idea of the total volume of gaps and cavities being retained even after crystallization to cubic ice or hexagonal ice is of importance also for the cryoflotation study reported here. It implies that hexagonal ice crystallized from HGW samples shows a lower density than void-free hexagonal ice of density 0.934 g cm^{-3} . The reduction in density is caused by the voids, and therefore, the density difference between void-free and void-containing hexagonal ice can be used as a correction factor. By applying this correction factor, the density of void-free HGW (corrected values in Table 2) can be calculated from the density of HGW containing voids (as-measured values in Table 2). To this end, we have converted HGW to hexagonal ice

Table 3. Densities of Low-Density Amorphous Ice (LDA) Samples as-measured by Cryoflotation in Liquid N₂/Ar^a

| LDA density (as-measured) | ice I _h Density | LDA density (corrected) |
|---------------------------|----------------------------|-------------------------|
| 0.935 | 0.932 | 0.937 |
| 0.930 | 0.926 | 0.938 |
| 0.929 | 0.928 | 0.935 |
| | | 0.937 ± 0.002 |

^a Reproducibility is ±0.005 g cm⁻³. The samples were converted to hexagonal ice by keeping them for 15 minutes at 260 K. See text for details.

by keeping it for 15 min at 260 K and measured the density of the resulting hexagonal ice by cryoflotation. These densities and the corrected densities for HGW samples containing no voids are given in Table 2 and plotted in Figure 4. Indeed, the corrected densities no longer depend on the aperture size and/or droplet size employed in the preparation procedure. They are constant within ±0.004 g cm⁻³. The density of hyperquenched glassy water at 80 K is determined to be 0.944 ± 0.005 g cm⁻³. This value is slightly higher than the density of hexagonal ice (0.932 ± 0.002 g cm⁻³) at the same temperature. The difference on the order of 0.01 g cm⁻³ is evident also in Table 2 when comparing the HGW density (as-measured) with the ice I_h density.

The density of bulk HGW determined here equals the density of vapor-deposited water (amorphous solid water, ASW), which was determined using the technique of buoyancy in liquid oxygen⁵² to be 0.94 ± 0.02 g cm⁻³ and optical interferometry and microbalance techniques to be 0.94 ± 0.01 g cm⁻³.^{87,88} Just like in the case of HGW, also in the case of ASW, voids may reduce the density, and also, the size of the reduction depends on the preparation history. For instance, Kay et al. have determined a highly angle of incidence dependent thin-film ASW sample density of 0.16–0.94 g cm⁻³ and porosities up to 80%,^{88–90} and Westley et al. have found a thin-film ASW density of 0.82 g cm⁻³ and a porosity of 0.13.⁹¹ Whereas the pores are of microscopic dimensions in the case of ASW and suitable for the adsorption of large amounts of small molecules like N₂,^{92–97} the cavities are much larger (micrometer-sized) in the case of HGW. Whereas the pores can be removed by annealing at, for example, 130 K in the case of ASW,^{97,98} the cavities remain in HGW even at 270 K, after crystallization to hexagonal ice. The densities of the ASW samples deposited at very low temperature may be significantly higher and determined from X-ray diffraction experiments to be, for example, 1.1 ± 0.1 g cm⁻³.^{19,26}

Low-Density Amorphous Ice (LDA). LDA prepared by heating uHDA is known to show the same radial density function as HGW,^{99,100} and therefore, the same density is expected for LDA and HGW. However, appearance of large voids resulting in the course of the preparation of LDA in the piston cylinder apparatus is unlikely. This hypothesis of practically void-free LDA samples is tested by converting the LDA samples to hexagonal ice by keeping them for 15 min at 260 K. Indeed, the densities of hexagonal ice samples crystallized from LDA are much closer to the density of void-free hexagonal ice, even though they tend to fall below the void-free hexagonal ice density slightly (see Table 3). We interpret this slight difference by some small microcracks, which may appear in the cylindrical samples when decompressing the sample to ambient pressure at 77 K.⁷⁰ The LDA density is determined to be 0.937 ± 0.002 g cm⁻³ at 80 K here after correction. This value is slightly lower than the

Table 4. Densities of Cubic Ice Samples Prepared by Hyperquenching of Micrometer-Sized Liquid Droplets to 170 K as-measured by Cryoflotation in Liquid N₂/Ar^a

| aperture/droplet diameter | ice I _c density (as-measured) | ice I _h density | ice I _c density (corrected) |
|---------------------------|--|----------------------------|--|
| 300 μm/3 μm | 0.901 | 0.895 | 0.940 |
| 300 μm/5 μm | 0.924 | 0.915 | 0.943 |
| | 0.925 | (0.905) | (0.954) |
| 400 μm/5 μm | 0.911 | 0.905 | 0.940 |
| | 0.911 | 0.898 | 0.947 |
| | 0.910 | 0.901 | 0.943 |
| | | | 0.943 ± 0.004 |

^a Reproducibility is ±0.005 g cm⁻³. One outlier was not considered for calculating the average value. The samples were converted to hexagonal ice by keeping them for 15 minutes at 260 K. Correction is necessary because samples contain a varying number of gaps and cavities in between droplet-shaped particles of cubic ice. See text for details. Entries in single lines represent averages from one sample preparation. Single pieces from the samples were floated up to three times. Different samples prepared in the same way are not included in the averages but are listed separately.

HGW density (Table 2) but slightly higher than the hexagonal ice density (Table 1).

Cubic Ice (I_c). Cubic ice samples prepared by hyperquenching liquid droplets were also investigated as a function of the aperture diameter and droplet size. In essence, the same trends as also noted in the case of HGW samples can be found again for cubic ice. Namely, smaller droplets and larger apertures result in more open aggregates of droplets containing more volume of cavities. By transformation to hexagonal ice and by applying the void correction, the densities of cubic ice become independent of experimental parameters employed in the course of sample preparation. Interestingly, the density of cubic ice of 0.943 ± 0.004 g cm⁻³ is identical to the HGW density and is higher than the hexagonal ice density by about 0.01 g cm⁻³. This can be clearly seen when comparing the ice I_c densities (as-measured) and the ice I_h densities in Table 4. By contrast to our finding, a slightly lower density (see Table 1) of the cubic form of ice is implied from high-resolution neutron powder diffraction studies.⁵⁷ The early results by Lisgarten and Blackman^{84,85} and Kumai⁸³ using electron diffraction, however, show a slightly higher density of cubic ice. We note, though, that the crystallographic cubic ice density in Table 1 refers to cubic ice prepared by heating ice II,⁵⁷ whereas we use the hyperquenching technique. Different routes of cubic ice preparation are known to result in different numbers of hexagonal stacking faults^{58,101} and different enthalpies of conversion to hexagonal ice.^{102,103} The hypothesis arising from the present study is that differing numbers of stacking faults may result in slightly different densities. A thorough study employing a range of preparation techniques for cubic ice is necessary in order to establish whether this hypothesis is justified.

Amorphous Ices at $\rho > 1 \text{ g cm}^{-3}$. Densities measured by cryoflotation were reported in earlier work for VHDA,⁶⁴ uHDA,⁶⁴ and HDA relaxed by decompressing VHDA at 140 K to 0.07 GPa (HDA, 0.07 GPa).⁷⁰ These data are depicted in Figure 5 together with the LDA data point (Table 3) and another form of relaxed HDA prepared by decompressing VHDA at 140 K to 0.20 GPa (HDA, 0.20 GPa).⁶³ The density measured by

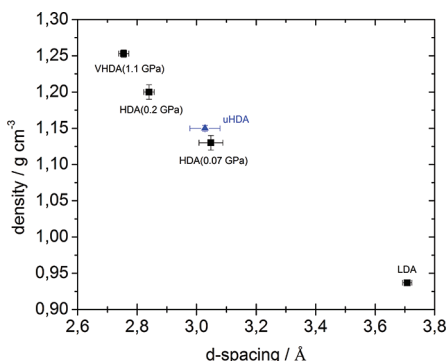


Figure 5. Correlation between the d spacing of first broad halo peak and density. The position of the first broad halo peak has been extracted by fitting a Lorentzian to powder X-ray diffractograms recorded on a Siemens D5000 diffractometer ($\text{Cu K}\alpha_1$) in $\theta-\theta$ arrangement at ~ 85 K using an Anton-Paar chamber and a Goebel mirror. Black squares refer to samples prepared by decompressing VHDA at 140 K,⁶³ where the pressure of quenching is indicated in parentheses. The blue triangle refers to pressure-amorphized hexagonal ice at 77 K.¹⁰⁹ Error bars are indicative of the reproducibility.

cryoflotation is plotted in Figure 5 against the d spacing of the first broad halo peak in powder X-ray diffractograms. The position of this halo peak is determined by fitting the diffractogram with single Lorentzian functions. Error bars include both the ambiguity in fitting the halo peak and the reproducibility when comparing different samples prepared in the same way. The plot shows, as expected, a clear correlation, where an increase in d spacing corresponds to a decrease in density. Interestingly, the density of uHDA is higher by 0.02 g cm^{-3} compared to the density of HDA (0.07 GPa), even though the positions of the first broad halo peak and all radial distribution functions are practically identical.⁷⁰ The density of a HDA sample relaxed at 140 K and 0.07 GPa is lower than the density of uHDA by 0.02 g cm^{-3} . This finding of an expanded nature was first inferred by Nelmes et al.,¹⁰⁴ and therefore, their use of the name “expanded” HDA (eHDA) is justified. However, a sample relaxed at 140 K and 0.20 GPa shows a density higher by 0.05 g cm^{-3} in comparison to uHDA. This is a reflection of the strained nature of uHDA and possibly also of the presence of structural inhomogeneities in uHDA undetectable by powder X-ray diffraction.^{105,106} In fact, it was even “proposed that, instead of being a homogeneously random structure, high-density amorphous ice may be a mixture of highly strained microcrystalline high-pressure phases of ice”.¹⁰⁷ However, after release of strain, the material might be homogeneous and unrelated to microcrystals. We, therefore, propose that the materials possibly related to the ultraviscous low-density liquid (LDL) and high-density liquid (HDL) postulated by Stanley and co-workers are LDA and HDA (0.07 GPa), respectively, but not uHDA.

■ DISCUSSION AND CONCLUSION

We present a method suitable for determining mass densities of solid samples in the density range of $0.81\text{--}1.40 \text{ g cm}^{-3}$. The method is based on density titration of a cryomixture of liquid argon and nitrogen and Archimedes’ principle. It yields densities at ambient pressure and $77\text{--}87$ K. Compared to other methods of density determination, our method has the advantage that instable samples can be studied, which transform, decompose, or melt above 100 K. Also, densities of amorphous samples can be determined accurately and precisely. Data collected on ice

polymorphs, including high-pressure polymorphs, show the reproducibility of the method to be $\pm 0.005 \text{ g cm}^{-3}$. Also, the uncertainty of the method is $\pm 0.005 \text{ g cm}^{-3}$ in the case of easily accessible samples of large crystal sizes such as hexagonal ice and naphthalene. In the case of high-pressure polymorphs, the difference from crystallographically determined densities, and hence uncertainty, typically amounts to $\pm 0.02 \text{ g cm}^{-3}$. The explanation for the increase in uncertainty is most likely sample preparation itself. Depending on the preparation protocol, powders of different grain sizes may be produced, and also, some contamination caused by parallel formation of a side-phase may affect the resulting density and may hamper comparison of densities obtained in different laboratories using different techniques. The excellent reproducibility and uncertainty in the case of easily accessible samples has clearly exceeded our expectations, while the uncertainty obtained in the case of high-pressure polymorphs corresponds to what we had expected beforehand.

The application of the techniques to a range of amorphous ice samples has revealed some interesting findings. In the case of HGW, we have found a clear trend of the density with the aperture size and the droplet size employed in the course of sample preparation. The decrease in density with aperture size and droplet size indicates the presence of an increasing volume of voids within the sample, which is inaccessible to liquid nitrogen and argon. By transforming the sample to hexagonal ice, the volume of the voids is retained, and therefore, the density difference between void-free and void-containing hexagonal ice can be employed for correction of the as-measured HGW density. The corrected HGW densities no longer depend on sample preparation details, and therefore, they reflect the microscopic bulk density of HGW. This density is found to be higher by 0.01 g cm^{-3} compared to the density of ice I_h. Similarly, the density of cubic ice prepared using the hyperquenching technique shows these trends with aperture size and droplet size. Also, the density of cubic ice is higher by 0.01 g cm^{-3} compared to the density of ice I_h. In the previous literature, it has been unclear whether the density of cubic ice is slightly higher or lower than the density of hexagonal ice. We speculate that differing cubicity indices for cubic ices of different preparation history are at the origin of the difference to the study of cubic ice prepared from ice II.⁵⁷ The density data for quench-recovered amorphous ices prepared in a piston cylinder apparatus show good correlation with the position of the first broad halo peak in diffraction experiments. However, the density of uHDA is significantly higher than the density of a relaxed form of HDA prepared by decompressing VHDA to 0.07 GPa at 140 K, despite the practically identical position of the halo peak and radial distribution functions.⁷⁰ We suggest that this reflects the strained nature of uHDA, whereas we suggest the relaxed form of HDA to be in metastable equilibrium (see also ref 108 in this issue), which is called eHDA by Nelmes et al.¹⁰⁴ If there is a HDA form, which can be regarded as the amorphous low-temperature proxy of the ultraviscous HDL postulated by Stanley and co-workers, then it has to be the relaxed form, but not the strained form.

■ AUTHOR INFORMATION

Corresponding Author

*E-mail: thomas.loerting@uibk.ac.at.

Notes

[§]Deceased March 13, 2011.

■ ACKNOWLEDGMENT

We are thankful to the Austrian Science Fund (K.W. Hertha-Firberg fellowship, T.L. START-award Y391) and the European Research Council (T.L. ERC Starting Grant SULIWA) for financial support.

■ REFERENCES

- (1) Stanley, H. E. *Introduction to Phase Transitions and Critical Phenomena*; Oxford University Press: New York, 1971.
- (2) Wagner, W.; Kleinrahm, R.; Loesch, H. W.; Watson, J. T. R.; Majer, V.; Padua, A. A. H.; Woolf, L. A.; Holste, J. C.; Palavra, A. M. D. F.; Fujii, K.; Stansfeld, J. W. *Exp. Thermodyn.* **2003**, *6*, 125.
- (3) Wagner, W.; Kleinrahm, R. *Metrologia* **2004**, *41*, S24.
- (4) Ridgely, C. T. *Eur. J. Phys.* **2010**, *31*, 419.
- (5) Klimeck, J.; Kleinrahm, R.; Wagner, W. *J. Chem. Thermodyn.* **1998**, *30*, 1571.
- (6) Glos, S.; Kleinrahm, R.; Wagner, W. *J. Chem. Thermodyn.* **2004**, *36*, 1037.
- (7) Richter, M.; Kleinrahm, R.; Glos, S.; Wagner, W.; Span, R.; Schley, P.; Uhrig, M. *Int. J. Thermophys.* **2010**, *31*, 680.
- (8) Kell, G. S.; Whalley, E. *J. Chem. Phys.* **1975**, *62*, 3496.
- (9) Kell, G. S.; McLaurin, G. E.; Whalley, E. *Proc. R. Soc. London, Ser. A* **1978**, *360*, 389.
- (10) Jarne, C.; Rivollet, F.; Richon, D. *J. Chem. Eng. Data* **2011**, *56*, 84.
- (11) Hidnert, P.; Peffer, E. L. *Density of solids and liquids*; U.S. Government Printing Office: Washington, DC, 1950.
- (12) Almeida, S. P.; Crouch, T. H. *Rev. Sci. Instrum.* **1971**, *42*, 1344.
- (13) Langen, M.; Hibiya, T.; Eguchi, M.; Egry, I. J. *J. Cryst. Growth* **1998**, *186*, 550.
- (14) Higuchi, K.; Kimura, K.; Mizuno, A.; Watanabe, M.; Katayama, Y.; Kurabayashi, K. *Meas. Sci. Technol.* **2005**, *16*, 381.
- (15) McLinden, M. O.; Loesch-Will, C. *J. Chem. Thermodyn.* **2007**, *39*, 507.
- (16) Mantilla, I. D.; Cristancho, D. E.; Ejaz, S.; Hall, K. R.; Atilhan, M.; Iglesias-Silva, G. A. *J. Chem. Eng. Data* **2010**, *55*, 4611.
- (17) Atilhan, M.; Aparicio, S.; Ejaz, S.; Cristancho, D.; Hall, K. R. *J. Chem. Eng. Data* **2011**, *56*, 212.
- (18) Kurzyniec, E.; Senkowski, T. *Zesz. Nauk. Uniw. Jagiellon., Ser. Nauk Mat. Przyrod.* **1958**, No. 4, 213.
- (19) Searls, M. G.; Rice, S. A. Amorphous Solid Water and Its Relationship to Liquid Water: A Random Network Model for Water. In *Water, a Comprehensive Treatise*; Franks, F., Ed.; Plenum Press: New York, 1982; Vol. 7, pp 83.
- (20) Eggert, J. H.; Weck, G.; Loubeyre, P.; Mezouar, M. *Phys. Rev. B: Condens. Matter Mater. Phys.* **2002**, *65*, 174105/1.
- (21) Hong, X.; Shen, G.; Prakapenka, V. B.; Rivers, M. L.; Sutton, S. R. *Rev. Sci. Instrum.* **2007**, *78*, 103905/1.
- (22) Sato, T.; Funamori, N. *Rev. Sci. Instrum.* **2008**, *79*, 073906/1.
- (23) Burton, E. F.; Oliver, W. F. *Proc. R. Soc. London, Ser. A* **1935**, *153*, 166.
- (24) Burton, E. F.; Oliver, W. F. *Nature* **1935**, *135*, 505.
- (25) Olander, D. S.; Rice, S. A. *Proc. Natl. Acad. Sci. U.S.A.* **1972**, *69*, 98.
- (26) Venkatesh, C. G.; Rice, S. A.; Narten, A. H. *Science* **1974**, *186*, 927.
- (27) Dubochet, J.; Adrian, M.; Vogel, R. H. *CryoLetters* **1983**, *4*, 233.
- (28) Mayer, E.; Pletzer, R. *J. Chem. Phys.* **1984**, *80*, 2939.
- (29) Klinger, J. *J. Phys., Colloq.* **1985**, *65*.
- (30) Jenniskens, P.; Blake, D. F. *Science* **1994**, *265*, 753.
- (31) Jenniskens, P.; Blake, D. F.; Wilson, M. A.; Pohorille, A. *Astrophys. J.* **1995**, *455*, 389.
- (32) Poole, P. H.; Sciortino, F.; Essmann, U.; Stanley, H. E. *Nature* **1992**, *360*, 324.
- (33) Poole, P. H.; Essmann, U.; Sciortino, F.; Stanley, H. E. *Phys. Rev. E* **1993**, *48*, 4605.
- (34) Poole, P. H.; Sciortino, F.; Essmann, U.; Hemmati, M.; Stanley, H. E.; Angell, C. A. *NATO Adv. Study Inst. Ser., Ser. C* **1994**, *435*, 53.
- (35) Stanley, H. E.; Angell, C. A.; Essmann, U.; Hemmati, M.; Poole, P. H.; Sciortino, F. *Physica A* **1994**, *206*, 1.
- (36) Sciortino, F.; Essmann, U.; Poole, P. H.; Stanley, H. E. Physical Chemistry of Aqueous Systems: Meeting the Needs of Industry. *Proceedings of the International Conference on the Properties of Water and Steam*, 12th; Orlando, FL, Sept. 11–16, 1994, 1995; p 355.
- (37) Sastry, S.; Debenedetti, P. G.; Sciortino, F.; Stanley, H. E. *Phys. Rev. E* **1996**, *53*, 6144.
- (38) Harrington, S.; Zhang, R.; Poole, P. H.; Sciortino, F.; Stanley, H. E. *Phys. Rev. Lett.* **1997**, *78*, 2409.
- (39) Mishima, O.; Stanley, H. E. *Nature* **1998**, *396*, 329.
- (40) Mishima, O.; Stanley, H. E. *Nature* **1998**, *392*, 164.
- (41) Stanley, H. E. *Pramana* **1999**, *S3*, S3.
- (42) Stanley, H. E.; Buldyrev, S. V.; Canpolat, M.; Mishima, O.; Sadr-Lahijany, M. R.; Scala, A.; Starr, F. W. *Phys. Chem. Chem. Phys.* **2000**, *2*, 1551.
- (43) Stanley, H. E.; Buldyrev, S. V.; Giovambattista, N.; La Nave, E.; Scala, A.; Sciortino, F.; Starr, F. W. Unsolved problems of liquid water. In *New Kinds of Phase Transitions: Transformations in Disordered Substances*; NATO Science Series; Brazhkin, V. V., Buldyrev, S. V., Ryzhov, V. N., Stanley, H. E., Eds.; Kluwer Academic Publishers: Dordrecht, The Netherlands, 2002; Vol. 81; p 309.
- (44) Buldyrev, S. V.; Stanley, H. E. *Physica A* **2003**, *330*, 124.
- (45) Giovambattista, N.; Eugene Stanley, H.; Sciortino, F. *Phys. Rev. E* **2005**, *72*, 031510.
- (46) Xu, L.; Kumar, P.; Buldyrev, S. V.; Chen, S.-H.; Poole, P. H.; Sciortino, F.; Stanley, H. E. *Proc. Natl. Acad. Sci. U.S.A.* **2005**, *102*, 16558.
- (47) Franzese, G.; Stanley, H. E. Understanding the Unusual Properties of Water. In *Water and Life: The Unique Properties of Water*; Lynden-Bell, R. M., Morris, S. C., Barrow, J. D., Finney, J. L., Harper, C., Ed.; Taylor & Francis: New York, 2006.
- (48) Kumar, P.; Buldyrev, S. V.; Becker, S. R.; Poole, P. H.; Starr, F. W.; Stanley, H. E. *Proc. Natl. Acad. Sci. U.S.A.* **2007**, *104*, 9575.
- (49) Xu, L.; Giovambattista, N.; Buldyrev, S. V.; Debenedetti, P. G.; Stanley, H. E. *J. Chem. Phys.* **2011**, *134*, 064507/1.
- (50) Handa, Y. P.; Mishima, O.; Whalley, E. *J. Chem. Phys.* **1986**, *84*, 2766.
- (51) Loerting, T.; Kohl, I.; Schustereder, W.; Hallbrucker, A.; Mayer, E. *ChemPhysChem* **2006**, *7*, 1203.
- (52) Ghormley, J. A.; Hochanadel, C. J. *Science* **1971**, *171*, 62.
- (53) Mishima, O.; Calvert, L. D.; Whalley, E. *Nature* **1984**, *310*, 393.
- (54) Muschick, W. *Glastech. Ber.* **1987**, *60*, 174.
- (55) Kohl, I.; Bachmann, L.; Hallbrucker, A.; Mayer, E.; Loerting, T. *Phys. Chem. Chem. Phys.* **2005**, *7*, 3210.
- (56) Kohl, I.; Mayer, E.; Hallbrucker, A. *Phys. Chem. Chem. Phys.* **2000**, *2*, 1579.
- (57) Kuhs, W. F.; Bliss, D. V.; Finney, J. L. *J. Phys., Colloq.* **1987**, *C1*, 631.
- (58) Hansen, T. C.; Koza, M. M.; Kuhs, W. F. *J. Phys.: Condens. Matter* **2008**, *20*, 285104/1.
- (59) Salzmann, C. G.; Loerting, T.; Klotz, S.; Mirwald, P. W.; Hallbrucker, A.; Mayer, E. *Phys. Chem. Chem. Phys.* **2006**, *8*, 386.
- (60) Loerting, T.; Kohl, I.; Salzmann, C.; Mayer, E.; Hallbrucker, A. *J. Chem. Phys.* **2002**, *116*, 3171.
- (61) Salzmann, C. G.; Kohl, I.; Loerting, T.; Mayer, E.; Hallbrucker, A. *Can. J. Phys.* **2003**, *81*, 25.
- (62) Salzmann, C. G.; Loerting, T.; Kohl, I.; Mayer, E.; Hallbrucker, A. *J. Phys. Chem. B* **2002**, *106*, 5587.
- (63) Winkel, K.; Elsaesser, M. S.; Mayer, E.; Loerting, T. *J. Chem. Phys.* **2008**, *128*, 044510/1.
- (64) Loerting, T.; Salzmann, C.; Kohl, I.; Mayer, E.; Hallbrucker, A. *Phys. Chem. Chem. Phys.* **2001**, *3*, 5355.
- (65) Röttger, K.; Endriss, A.; Ihringer, J.; Doyle, S.; Kuhs, W. F. *Acta Crystallogr.* **1994**, *B50*, 644.
- (66) Eisenberg, D.; Kauzmann, W. *The Structure and Properties of Water*; Oxford University Press: Oxford, U.K., 1969.

- (67) LaPlaca, S.; Post, B. *Acta Crystallogr.* **1960**, *13*, 503.
(68) Brill, R.; Tippe, A. *Acta Crystallogr.* **1967**, *23*, 343.
(69) *International critical tables of numerical data, physics, chemistry and technology*; McGraw-Hill: New York, 1928.
(70) Loerting, T.; Winkel, K.; Seidl, M.; Bauer, M.; Mitterdorfer, C.; Handle, P. H.; Salzmann, C. G.; Mayer, E.; Finney, J. L.; Bowron, D. T. *Phys. Chem. Chem. Phys.* **2011**, *13*, 8783.
(71) LaPlaca, S. J.; Hamilton, W. C.; Kamb, B.; Prakash, A. *J. Chem. Phys.* **1973**, *58*, 567.
(72) Kamb, B.; Prakash, A. *Acta Crystallogr., Sect. B* **1968**, *24*, 1317.
(73) Londono, J. D.; Kuhs, W. F.; Finney, J. L. *J. Chem. Phys.* **1993**, *98*, 4878.
(74) Kamb, B. *Science* **1965**, *150*, 205.
(75) Kamb, B.; Prakash, A.; Knobler, C. *Acta Crystallogr.* **1967**, *22*, 706.
(76) Kuhs, W. F.; Finney, J. L.; Vettier, C.; Bliss, D. V. *J. Chem. Phys.* **1984**, *81*, 3612.
(77) Kuhs, W. F.; Lobban, C.; Finney, J. L. *Rev. High Pressure Sci. Technol.* **1998**, *7*, 1141.
(78) Lobban, C.; Finney, J. L.; Kuhs, W. F. *J. Chem. Phys.* **2000**, *112*, 7169.
(79) Engelhardt, H.; Kamb, B. *J. Chem. Phys.* **1981**, *75*, 5887.
(80) Kohl, I.; Loerting, T.; Salzmann, C.; Mayer, E.; Hallbrucker, A. *NATO Sci. Ser., II* **2002**, *81*, 325.
(81) Koza, M.; Schober, H.; Tölle, A.; Fujara, F.; Hansen, T. *Nature* **1999**, *397*, 660.
(82) Kraus, W.; Nolze, G. *J. Appl. Crystallogr.* **1996**, *29*, 301.
(83) Kumai, M. *J. Glaciol.* **1968**, *7*, 95.
(84) Lisgarten, N. D.; Blackman, M. *Nature* **1956**, *178*, 39.
(85) Blackman, M.; Lisgarten, N. D. *Proc. R. Soc. London, Ser. A* **1957**, *239*, 93.
(86) Kamb, B. *Acta Crystallogr.* **1964**, *17*, 1437.
(87) La Spisa, S.; Waldheim, M.; Lintemoot, J.; Thomas, T.; Naff, J.; Robinson, M. *J. Geophys. Res. [Planets]* **2001**, *106*, 33351.
(88) Dohnalek, Z.; Kimmel, G. A.; Ayotte, P.; Smith, R. S.; Kay, B. D. *J. Chem. Phys.* **2003**, *118*, 364.
(89) Stevenson, K. P.; Kimmel, G. A.; Dohnalek, Z.; Smith, R. S.; Kay, B. D. *Science* **1999**, *283*, 1505.
(90) Kimmel, G. A.; Stevenson, K. P.; Dohnalek, Z.; Smith, R. S.; Kay, B. D. *J. Chem. Phys.* **2001**, *114*, 5284.
(91) Westley, M. S.; Baratta, G. A.; Baragiola, R. A. *J. Chem. Phys.* **1998**, *108*, 3321.
(92) Ghormley, J. A. *J. Chem. Phys.* **1967**, *46*, 1321.
(93) Mayer, E.; Pletzer, R. *Nature* **1986**, *319*, 298.
(94) Mayer, E.; Pletzer, R. *J. Phys., Colloq.* **1987**, *48*, 581.
(95) Rowland, B.; Fisher, M.; Devlin, J. P. *J. Chem. Phys.* **1991**, *95*, 1378.
(96) Devlin, J. P. *J. Phys. Chem.* **1992**, *96*, 6185.
(97) Ayotte, P.; Smith, R. S.; Stevenson, K. P.; Dohnalek, Z.; Kimmel, G. A.; Kay, B. D. *J. Geophys. Res. [Planets]* **2001**, *106*, 33387.
(98) Manca, C.; Martin, C.; Roubin, P. *Chem. Phys. Lett.* **2002**, *364*, 220.
(99) Bowron, D. T.; Finney, J. L.; Hallbrucker, A.; Kohl, I.; Loerting, T.; Mayer, E.; Soper, A. K. *J. Chem. Phys.* **2006**, *125*, 194502.
(100) Winkel, K.; Bowron, D. T.; Loerting, T.; Mayer, E.; Finney, J. L. *J. Chem. Phys.* **2009**, *130*, 204502.
(101) Hansen, T. C.; Falenty, A.; Kuhs, W. F. *Phys. Chem. Ice, [Proc. Int. Conf.]*, *11th 2007*, 201.
(102) Handa, Y. P.; Klug, D. D.; Whalley, E. *J. Chem. Phys.* **1986**, *84*, 7009.
(103) Johari, G. P.; Hallbrucker, A.; Mayer, E. *J. Phys. Chem.* **1990**, *94*, 1212.
(104) Nelmes, R. J.; Loveday, J. S.; Straessle, T.; Bull, C. L.; Guthrie, M.; Hamel, G.; Klotz, S. *Nat. Phys.* **2006**, *2*, 414.
(105) Schober, H.; Koza, M.; Tölle, A.; Fujara, F.; Angell, C. A.; Böhmer, R. *Physica B* **1998**, *241–243*, 897.
(106) Koza, M. M.; Geil, B.; Winkel, K.; Koehler, C.; Czeschka, F.; Scheuermann, M.; Schober, H.; Hansen, T. *Phys. Rev. Lett.* **2005**, *94*, 125506.
(107) Johari, G. P. *Phys. Chem. Chem. Phys.* **2000**, *2*, 1567.
(108) Winkel, K.; Mayer, E.; Loerting, T. *J. Phys. Chem. B* **2011**, DOI: 10.1021/jp203985w.
(109) Mishima, O.; Calvert, L. D.; Whalley, E. *J. Phys., Colloq.* **1984**, *C8*, 239.